

Lipid Bilayer Reorganization under Extreme pH Conditions

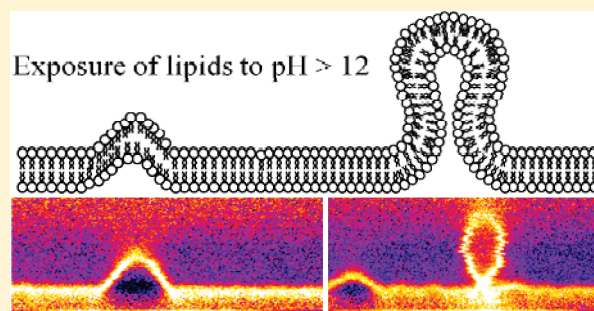
Matthew P. Goertz,^{*,†} Nikita Goyal,[‡] Gabriel A. Montano,[‡] and Bruce C. Bunker[†]

[†]Center for Integrated Nanotechnologies, Sandia National Laboratories, Albuquerque, New Mexico 87185, United States

[‡]Los Alamos National Laboratories, Los Alamos, New Mexico 87545, United States

S Supporting Information

ABSTRACT: Supported lipid bilayers containing phosphatidylcholine headgroups are observed to undergo reorganization from a 2D fluid, lipid bilayer assembly into an array of complex 3D structures upon exposure to extreme pH environments. These conditions induce a combination of molecular packing and electrostatic interactions that can create dynamic morphologies of highly curved lipid membrane structures. This work demonstrates that fluid, single-component lipid bilayer assemblies can create complex morphologies, a phenomenon typically only associated with lipid bilayers of mixed composition.



INTRODUCTION

Lipid membranes are essential and ubiquitous in living systems. Composed mainly of amphiphilic lipid molecules, these supermolecular assemblies create a barrier between the internal and external cellular environment as well as intracellular barriers between cellular compartments.¹ Membrane morphology and dynamics are of interest to a variety of fields in both biology and biomimetic materials. From a biological perspective, understanding membrane dynamics is essential to understanding biogenesis and the formation of cellular life. Understanding unique compositions of membranes is also critical to investigating how cellular components such as mitochondria² and chloroplasts³ create tight membrane curvatures, a condition often necessary for proper function. Further, from a biomimetic view, many biosensors are based on the principle of recognition by cellular receptors inserted into membranes.⁴ It is critical in such sensing applications to understand how exposure to various environments can affect the composition, structure, and function of the biosensing platform.

In many respects, the easiest mechanism for investigating membrane morphology and dynamics is to study model membrane systems known as lipid bilayer assemblies (LBA). Such assemblies can vary in composition from a single lipid component to complex assemblies of mixed lipids and membrane-associated molecules such as proteins. Physical properties of the LBA such as membrane fluidity, charge, curvature, and phase separation/domain formation can be tuned by varying its chemical composition.⁵ In this work, we investigate how physical properties and resulting morphology of a single-component phospholipid LBA change in response to exposure to extreme pH environments.

As mentioned above, 3D lipid structures are seen throughout biology. Typically, such structures are thought to form via local concentrations of curve-forming lipids and or proteins that can

induce such structures. While this is likely true in the natural world, the potential to form such structures in single component systems exists. Further, prebiotic conditions, in which initial processes of cellular formation occurred, such as membrane compartmentalization, likely took place at drastically different environments, including relatively high pH and minimal components.⁶ Previous work by Hovis and others have shown the ability to create 3D LBA structures from formed lipid bilayer assemblies using multicomponent lipid mixtures, some of which are similar to those presented in this work.^{7,8} However, this work represents, to our knowledge, the first example of 3D lipid membrane rearrangements of a fluid LBA consisting of a single lipid component using a simple change in pH. Here, we show that it is possible to create a variety of structures and dynamics responses in 1-palmitoyl-2-oleoyl-*sn*-glycero-3-phosphocholine (POPC) lipid membranes as a function of pH. We are able to visualize processes such as vesicle budding and delamination from 2D LBAs and create both dynamic and stable 3D components such as bubbles and invaginations of various size and complexity. This work represents a potential mechanism for synthesizing new lipid structures while maintaining a desired functionality. Lastly, as will be described, a potential mechanism for creating unsupported LBAs is shown that would be beneficial in our ability to investigate membrane-associated protein structure–function relationships.

METHODS AND MATERIALS

Materials. All lipids and fluorescence dyes were purchased in dry powdered form. 1-Palmitoyl-2-oleoyl-*sn*-glycero-3-phosphocholine (POPC) and 1,2-distearoyl-*sn*-glycero-3-phosphocholine (DSPC) were purchased from Avanti Polar Lipids (Alabaster, AL). 2-(4,4-Difluoro-

Received: January 11, 2011

Revised: March 10, 2011

Published: April 04, 2011

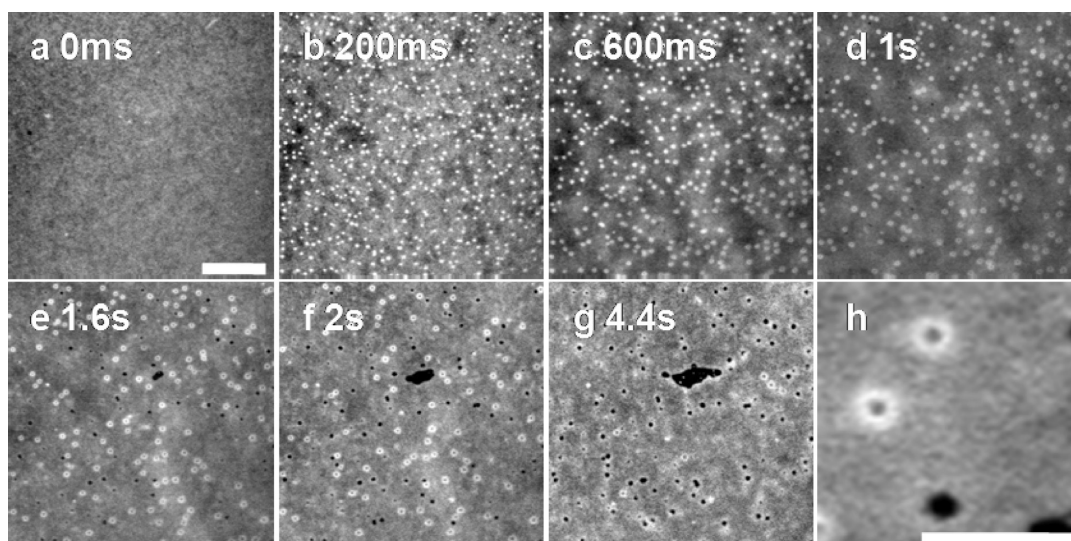


Figure 1. Epifluorescence images of a POPC bilayer exposed to pH 1. Panels a–g show the time evolution of cap formation and removal (for a–g, the scale bar represents $10\ \mu\text{m}$). Panel h shows a zoomed in image of features in panel f (for h, the scale bar represents $2\ \mu\text{m}$).

5,7-dimethyl-4-bora-3a,4a-diaza-*s*-indacene-3-dodecanoyl)-1-hexadecanoyl-*sn*-glycero-3-phosphocholine (C_{12} -Bodipy-PC) and Texas Red 1, 2-dihexadecanoyl-*sn*-glycero-3-phosphoethanolamine, triethylammonium salt (Texas Red DHPE), were purchased from Molecular Probes (Eugene, OR). Both lipids (POPC, DSPC) and dye (C_{12} -Bodipy-PC, Texas Red DHPE) were used as received without further purification and dissolved in chloroform (HPLC grade). All buffers, acids, and bases were made using $18\ \text{M}\Omega\ \text{cm}\ \text{H}_2\text{O}$ (Barnstead Nanopure filter).

Liposome and Supported Lipid Bilayer Formation. Liposomes were prepared by probe sonication. Briefly, lipids containing 0.5 mol % dye were dried from chloroform overnight under vacuum and rehydrated in pH 7.4 PBS buffer solutions. The lipid suspension was subjected to three freeze–thaw cycles and sonicated for 10 min using a probe sonicator. Liposomes of POPC were kept at $3\ ^\circ\text{C}$ and used within 10 days. Liposomes of DSPC were stored at $60\ ^\circ\text{C}$ and used within 1 day. Supported lipid bilayers were deposited by placing liposomes on a UV–ozone cleaned glass coverslip and incubating for 10 min. Excess liposomes were removed by exchanging the buffer solution at least 10 times. Incubation was performed at room temperature and $60\ ^\circ\text{C}$ for POPC and DSPC, respectively.

Microscopy of Supported Lipid Bilayer Reorganization. Lipid bilayer rearrangement was imaged with a combination of epifluorescence microscopy, confocal fluorescence microscopy, and atomic force microscopy (AFM). All fluorescence microscopy was conducted with an Olympus IX-71 inverted microscope using a $100\times$ oil immersion objective. This setup produced images with a size of $130 \times 100\ \mu\text{m}$. Epifluorescence microscope used a mercury arc lamp, Hamamatsu OrcaII-erg camera with resolution of 1344×1032 pixels, and an Olympus U-MWIBA3 filter set for imaging. All epifluorescence images were acquired with a 30% transmittance neutral density filter to minimize photobleaching. Confocal fluorescence microscopy used a spinning disk setup produced by Intelligent Imaging Innovations (Denver, CO), a Nano-F piezo actuated objective from Mad City Laboratories (Madison, WI), and a Photometrics CoolSNAP_{HQ} camera with a resolution of 696×520 pixels for imaging. Atomic force microscopy used a Molecular Imaging (now Agilent Technologies) Picoscan 2500 with magnetic-ac (MAC) mode. MAC mode cantilevers (type II, resonant frequency $\sim 24\ \text{kHz}$ in water) were purchased from Agilent Technologies (Englewood, CO). All images, except for fluorescence recovery after photobleaching (FRAP) experiments, have been brightness and contrast adjusted for visual clarity.

Exposure of a Lipid Bilayer to Extreme pH Changes. The effect of extreme pH changes on POPC lipid bilayers was observed by first creating a supported lipid bilayer on a glass coverslip in pH 7.4 PBS buffer as described above. The glass coverslip is held in a fluid cell with $\sim 600\ \mu\text{L}$ of solution and designed to allow both fluorescence imaging and AFM of a single sample. In each experiment the bilayer was initially rinsed with H_2O and then the solution volume above the bilayer was decreased to a minimum amount ($\sim 100\ \mu\text{L}$) without dehydrating the surface. Subsequently, $500\ \mu\text{L}$ of new solution (acid, HCl/base, NaOH) was pipetted onto the bilayer, and its effects were observed. The addition of the new acid/base solution was performed with the coverslip and fluid cell already mounted and aligned on the microscope; therefore, time 0 as described in the results indication is a close approximation to pH adjustment.

RESULTS

Exposure to Acidic pH. Figure 1 shows epifluorescence images of the time evolution of reorganization of a POPC bilayer exposed to pH 1. Before treatment, the bilayer appears as a uniform intensity image. As the pH of the solution above the bilayer decreases by addition of pH 1 HCl, several features appear in/on the bilayer. The speed at which we were able to observe changes in the bilayer is limited by the acquisition time of the camera needed to produce quality images, (~ 200 – $500\ \text{ms}$). In the first image acquired after the bilayer is exposed to pH 1 (200 ms, Figure 1b) several small bright features appear. By 600 ms after exposure to pH 1 the number of bright features decrease and the remaining features appear to increase in size. From 600 ms to $\sim 5\ \text{s}$ (Figure 1c–g) several processes are observed to occur simultaneously. First, the bright objects created immediately after exposure to pH 1 follow one of two possible paths. The bright objects either disappear as they are absorbed into the bilayer or they begin to appear as caps that grow to a critical size of 1 – $2\ \mu\text{m}$ in diameter before they break away from the surface, leaving a circular dark spot behind. A movie of this process is provided in the Supporting Information. Figure 1h shows a zoomed image of two lipid caps and a dark spot left after one of the ring structures left the surface. By raising the focus of the microscope to above the bilayer, we observed that the liposomes

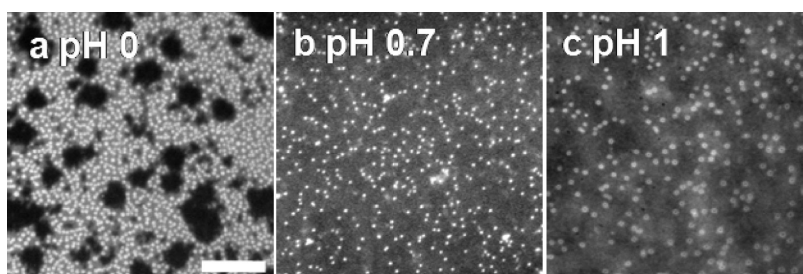


Figure 2. Epifluorescence of exposure of a POPC bilayer to acidic conditions. Images taken 1 s after exposure to pH 0, 0.7, and 1 are shown in panels a, b, and c, respectively (the scale bar represents 10 μm).

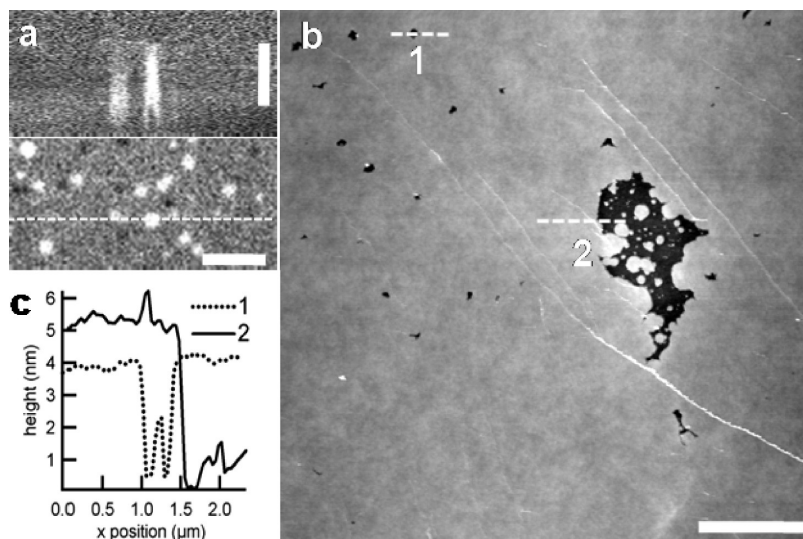


Figure 3. Confocal fluorescence (a) and AFM (b and c) of a POPC bilayer after exposure to pH 1. Panel a shows the topography of caps formed after 1 min exposure to pH 1. Several caps and holes are shown in a single z-slice [for a (bottom), the scale bar represents 10 μm]. Cap height is shown in a 3D reconstruction taken along the x - y slice marked by white dashed line. The reconstruction was acquired through z-series with 0.02 μm spacing [for a (top), the scale bar to indicate height represents 2 μm and the x scale is preserved from the bottom image]. Panel b shows an AFM topography image of the holes remaining after 15 min exposure to pH 1 (for b, the scale bar represents 5 μm). Portions of topographic linescans of slices labeled 1 and 2 are shown in panel c.

that have detached from the surface remain suspended in solution. Another type of feature created are large dark patches, 5–10 μm in size, that are irregularly shaped. An example of this is shown in the center of Figure 1e–g. Note that creation of membrane patches lags the formation of smaller bright features by ~ 1 –2 s. Repetition of this experiment revealed that the time scale for creation of the features shown in Figure 1 varies from several seconds to ~ 2 min. While there is variation in time scales for each sample, the general trends and features are reproducible. We find that after 2 min of exposure to pH 1 nearly all of the lipid caps have either been readsorbed or left the surface. Note that both the lipid caps and irregular membrane patches have the capability to heal over several minutes to hours (see Recovery and Fluidity of pH-Treated Lipid Bilayer Assemblies).

The extent of low pH treatment of a POPC bilayer was examined by exposing bilayers to a solution with pH 2, 1, 0.7, and 0. At acidic pH values of 2 and above, we find that there is no modification of the bilayer, as epifluorescence microscopy reveals a featureless uniform intensity across each image (data not shown). Figure 2 shows the effect of exposure of a POPC bilayer to pH 0 (a), 0.7 (b), and 1 (c) after 1 s of treatment. The features and trends of acid exposure observed in Figure 1 persist at lower

pH, although at increased amounts and speed. Under the strongest acidic conditions used, pH 0, the entire bilayer is covered in either lipid caps or membrane patches.

In order to prove the formation of lipid caps and membrane observed in Figures 1 and 2, we examined our LBAs using both confocal fluorescence microscopy and AFM. Figure 3a shows a confocal fluorescence micrograph of a POPC bilayer exposed to pH 1 for 1 min. The bottom panel is focused in the plane of the bilayer and shows several of the lipid caps. Instrumental resolution limits the clarity of the caps compared to the epifluorescence images of Figures 1 and 2. The 3D nature of the caps was probed by acquiring a series of images in which the focus was raised using a piezo mounted objective in 0.02 μm steps for a total travel of 2 μm . The top panel shows a 3D reconstruction of the caps marked by the horizontal dashed line in the bottom panel. The reconstruction shows that the cap imaged is a hemispherical cap that is ~ 2 μm in diameter.

The membrane patches are revealed by examining AFM topography images of the POPC bilayer after exposure to pH 1 for 15 min (Figure 3b). Topographic linescans shown in Figure 3c reveal that the height contrast of holes are 3–5 nm below the surface of the bilayer, corresponding to the thickness of

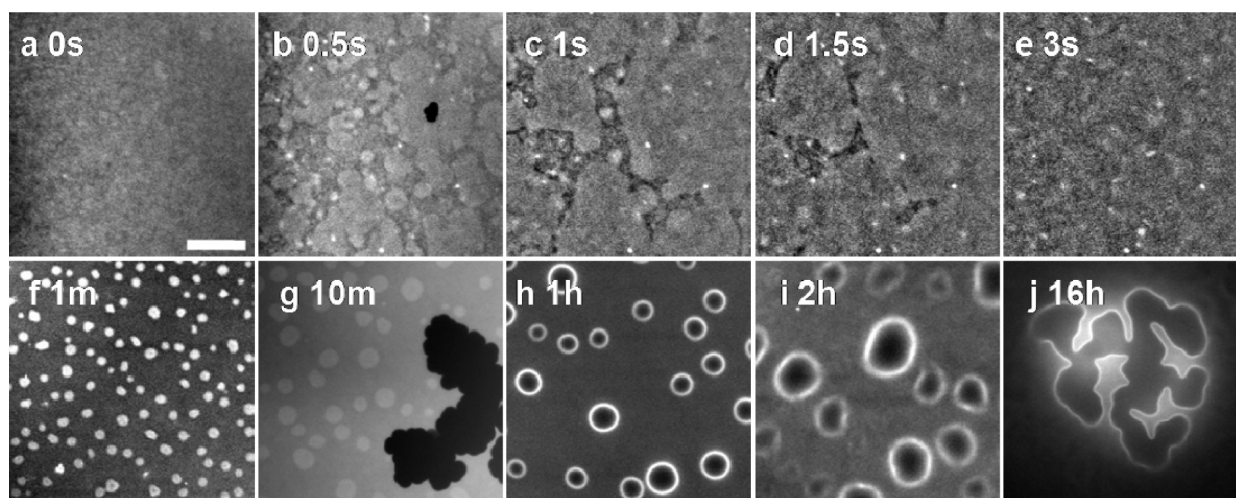


Figure 4. Epifluorescence images of a POPC bilayer exposed to pH 12.5. Panels a–j show the time evolution of bilayer delamination and reorganization (the scale bar represents 10 μm).

an individual POPC bilayer. The circular dark features correspond to holes left in the membrane after removal of a lipid cap, and the irregular patches are due to membrane disruption (see Discussion). Unfortunately we were unsuccessful in using AFM to image caps protruding from the bilayer surface. We believe that this is because the caps do not exhibit sufficient mechanical stability to be successfully imaged. Also note that while in Figure 1h the holes left behind as a cap left the surface are distinctly circular in shape, AFM images shows that these boundaries are irregular. We will later address this issue in regard to the ability of the bilayer to heal over longer time scales (see Discussion).

Exposure to Basic pH. Each of the experiments described above was also conducted with exposure of a POPC bilayer to basic pH solutions of NaOH. Figure 4 shows the time evolution for the reorganization of a bilayer to pH 13. It is clear that the range of surface features for basic treatment of POPC is more complex than for acidic exposure, and we identify three distinct behaviors of LBA rearrangement. The first observed behavior (Figure 4b–e) is growth of large patches of the bilayer that appear slightly brighter than the surrounding background. By 3 s after base treatment the light-colored patches grow, coalesce, and eventually cover the entire bilayer. We often observed that the larger light-colored patches as seen in Figure 4b have a dark spot at their center. This dark spot grows to several micrometers in diameter and then shrinks and often disappears within a few seconds. After the light-colored patches envelope the entire bilayer, it remains featureless for ~ 30 s to 1 min, upon which we observe the second distinct base-induced POPC LBA rearrangement. At a time scale of ~ 1 –10 min after base exposure we again observe the growth of bright and dark patches (Figure 4f,g). These bright patches begin with a uniform intensity across the entire feature and have two dynamic characteristics. First, the boundary between the bright patches and the rest of the bilayer is dynamic, as it fluctuates in a manner similar to a liquid/liquid phase coexistence boundary. Second, the bright patches have lateral mobility as they are observed to move within the bilayer and coalesce when two patches form intimate contact. A movie of the dynamic characteristics of these bright features is shown in the Supporting Information. Accompanying these bright patches is the growth and disappearance of dark patches

on the bilayer surface, as shown in Figure 4g. These dark features are irregularly shaped and are often formed and destroyed within a few seconds. They are also fairly sparse on the surface and we must actively search over several millimeters to find them. An example movie of the time scale at which a dark feature can disappear is provided in the Supporting Information. After a period of several minutes to ~ 1 h (Figure 4h), the membrane displays a final distinct behavior. During this time, lipid caps in the bilayer begin to appear. These caps look similar to those in Figure 1, except that they are larger and are never observed to break away or disappear into the bilayer. At time scales of several hours the caps continue to merge and grow in size, becoming irregularly shaped. Figure 4j shows that by 16 h after base exposure the number of features on the bilayer surface has decreased significantly and has become irregularly shaped; however, they continue to maintain a bright boundary at their edges. Similar to our observations with acidic treatments of POPC, we observe that there are variations in the time scale needed to produce the features shown in Figure 4. It may take up to 30 s for the initial bright patches to envelope the entire surface. Similarly, the coalescence of ring-shaped structures formed at longer time scale occurs within 10 min to 2 h.

We have examined the range of basic pH values that will produce the features observed in Figure 4 by incrementally increasing the pH until we observe changes in the bilayer. At basic pH values of ≤ 11 we do not observe any changes in a POPC bilayer (images not shown). In the first seconds after exposure of bilayers to pH values of 12, 12.5, or 13, the features observed in Figure 4a–e are observed. However, at longer time scales epifluorescence images reveal a difference between exposure to pH 12 versus 12.5 and 13 (Figure 5). At pH 12, the reorganization of a POPC bilayer ceases after a few seconds (Figure 5a) and featureless bilayers remain. While a few membrane patches are created, we never observe the features shown in Figure 4f–j. If the bilayer is exposed to pH values of 12.5 or 13, Figure 5b,c shows the bright features that appear at longer time scales.

Similar to our investigation of acidic treatment of POPC bilayers, confocal fluorescence microscopy and AFM are used to resolve the features produced with basic pH. Figure 6a shows a single frame of a z-series after exposure of POPC to pH 13 for 15 min. At the level of

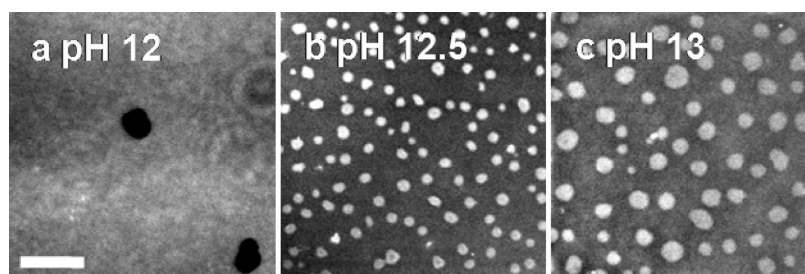


Figure 5. Epifluorescence images of a POPC bilayer exposed to basic conditions. Images taken 1 min after exposure to pH 12, 12.5, and 13 are shown in panels a, b, and c, respectively (the scale bar represents $10\ \mu\text{m}$).

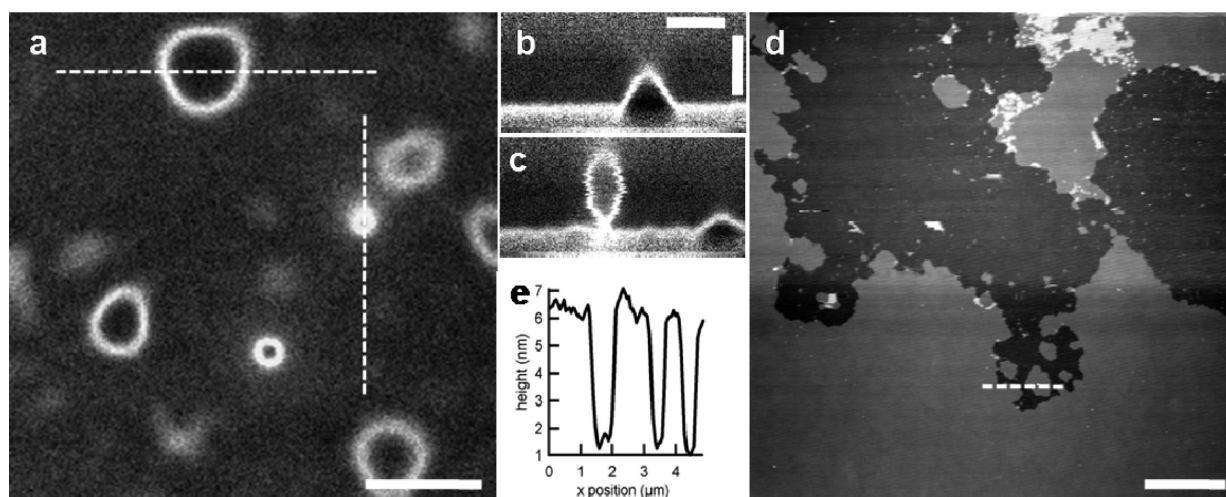


Figure 6. Confocal fluorescence (a–c) and AFM (d and e) of a POPC bilayer after exposure to pH 13 for 15 min. Panel a shows a single z-slice of several half and fully spherical caps (a scale bar represents $10\ \mu\text{m}$). Cap height and geometry are shown in 3D reconstructions taken along the x – y slices marked horizontally (b) and vertically (c). The reconstructions were acquired through z-series with $0.1\ \mu\text{m}$ spacing (for b and c, the vertical scale bar represents $5\ \mu\text{m}$ and the horizontal scale bar represents $10\ \mu\text{m}$). Panel d shows an AFM topography image of the holes remaining after 15 min exposure to pH 13 (for d, the scale bar represents $5\ \mu\text{m}$). Topographic linescans of the slice shown with a white dashed line is shown in panel e.

the bilayer surface, we observe both large ($\sim 5\ \mu\text{m}$ diameter) and small ($\sim 1\ \mu\text{m}$ diameter) caps. Figure 6b shows a 3D reconstruction of the cap marked with the horizontal dashed line. The cap is similar in appearance to those formed through acid treatment in Figure 3a, though the larger size allows for easier visualization and interpretation. The shape of the cap in Figure 6a marked with the vertical dashed line is also reconstructed in Figure 6c. We observe this feature to be a spherically shaped bud that has grown from and is still attached to the bilayer.

AFM imaging of the dark patches observed in Figure 4g revealed these to be membrane disruptions in the bilayer (Figure 6d). As discussed later, the dynamic nature of the features as well as previously reports of dye segregation in biphasic lipid systems necessitated proving that the dark patches were membrane patches.⁷ Note that even though these are often dynamic, as they can grow and disappear within a few seconds, successful AFM imaging required trial and error to find a stationary feature. A topographic linescan of the area marked with a dashed line (Figure 6e) reveals the boundary of the dark feature to a $\sim 5\ \text{nm}$ depression, indicative of removal of a single POPC bilayer.

Recovery and Fluidity of pH-Treated Lipid Bilayer Assemblies. To examine the ability of a POPC bilayer to recover after acid-induced rearrangement, we observed the effects of acid at longer times than shown in Figure 1. At time scales of several minutes,

Figure 7 shows that we observe the complete healing of the holes remaining after cap detachment and slight healing of the larger membrane patches created during cap formation. Figure 7a,b shows epifluorescence images taken 1 min (a) and 45 min (b) after exposure of a POPC bilayer to pH 1. The majority of the small holes have healed within 45 min with only the larger membrane patches remaining. A higher resolution image of the healing process was acquired on the same sample with AFM (Figure 7c,d). The AFM image reveals that 15 min after exposure to pH 1 (Figure 7c) the micrometer-sized spherical holes in Figure 7a have begun to heal and are only $\sim 500\ \text{nm}$ in diameter. After 45 min of exposure to pH 1 (Figure 7d) nearly all of these holes have completely healed, leaving a fully intact bilayer. The sequence of Figure 7c,d also shows that the larger membrane patches have a tendency to heal, though we do not observe them to completely disappear within 16 h.

Investigation into the potential mechanism for how holes in a lipid bilayer could heal was done with two experiments. First, to test the hypothesis that detached lipid caps surface are adsorbing on the surface and filling the bilayer, we rinsed the bilayer several times with fresh pH 1 solution. After rinsing away the detached caps, the bilayer continues to heal over the course of $\sim 1\ \text{h}$ (data not shown). From this we conclude that the holes are not filling in from deposition of excess lipids in solution. We also tested the fluidity of the bilayer through a qualitative FRAP experiment. Figure 7e,f shows the

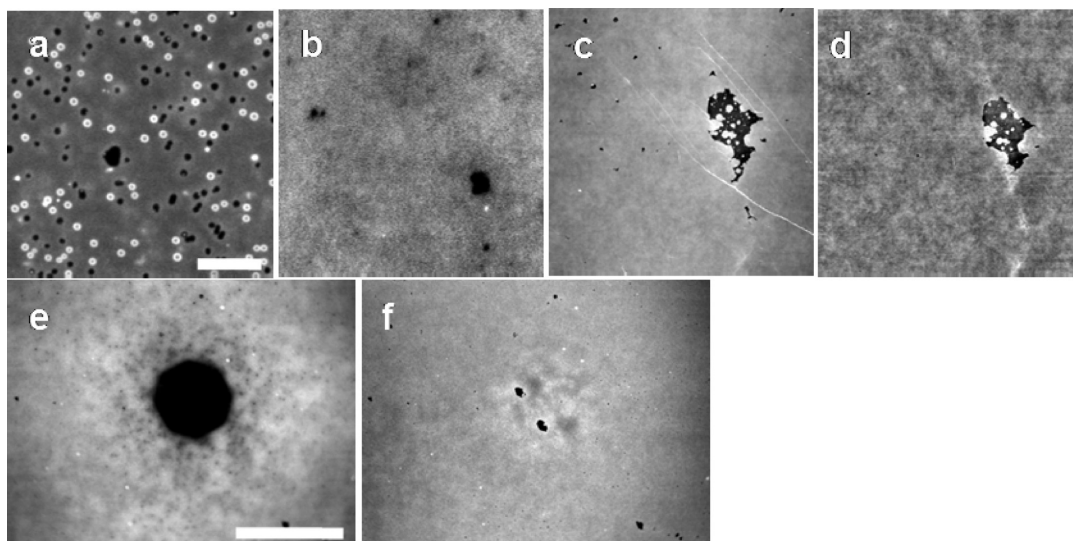


Figure 7. Epifluorescence (a and b), AFM (c and d), and FRAP (e and f) images of the recovery and fluidity of a POPC bilayer after exposure to pH 1. Healing of the small ($1\text{--}2\ \mu\text{m}$) holes is observed in both epifluorescence images taken 1 min (a) and 45 min (b) after pH 1 exposure, as well as AFM, taken at 15 min (c) and 45 min (d) (for a–d, the scale bar represents $10\ \mu\text{m}$). A FRAP experiment performed 45 min after exposure to pH 1 is shown at immediately after bleaching (e) and after 10 min of recovery (f) (for e and f, the scale bar represents $40\ \mu\text{m}$).

fluidity of a POPC bilayer exposed to pH 1 for 45 min. Note that the sample location for FRAP was chosen as it contained two irregularly shaped holes in the bilayer. Photobleaching a $\sim 40\ \mu\text{m}$ diameter spot was performed by removing the neutral density filter on the microscope and bleaching at full light intensity for 2 min. We observe that within 10 min after bleaching the bilayer fluorescence intensity is almost completely recovered, indicating that it remains fluid. We also performed several qualitative FRAP experiments on basic pH treated POPC bilayers. We observe the bilayer to *always* be fluid after exposure to basic pH up to 13 (data not shown).

Investigating Possible Factors of Reorganization. Several experiments were conducted in order to identify factors that influence acid/base-induced reorganization of a POPC bilayer. Understanding these factors, which include fluidity, reversibility/rinsing, fluorescent dye incorporation, and electrostatic forces, is essential in developing potential mechanisms of bilayer reorganization.

First, the role of fluidity on the ability of a bilayer to respond to both low and high pH environments was explored by switching the lipids in the bilayer from POPC to DSPC. We chose DSPC as a control because it has the same phosphatidylcholine (PC) headgroup and only differs from POPC in its acyl tails. While the unsaturated acyl tail on POPC lipids creates a fluid bilayer at room temperature, the fully saturated DSPC tails produce a gel-phase bilayer. Repeating our experiments by exposing a DSPC bilayer to solutions of pH 0–13 produced no observable change in bilayer appearance (data not shown). We therefore conclude that fluidity is a necessary factor for bilayer reorganization.

Reversibility, defined here as returning a bilayer back to its original flat configuration, was tested by exposing the bilayer to either acid or base and then rinsing with a pH 7.4 PBS buffer solution. Figure 8a,b shows that rinsing an acid-treated bilayer with PBS buffer produced little change within 1 min. We observed the two irregularly shaped holes in the center of Figure 8a to heal within 1 min. Drastically different results are observed in Figure 8c,d for rinsing of a POPC bilayer exposed to pH 13. After rinsing with neutral PBS buffer the base-treated

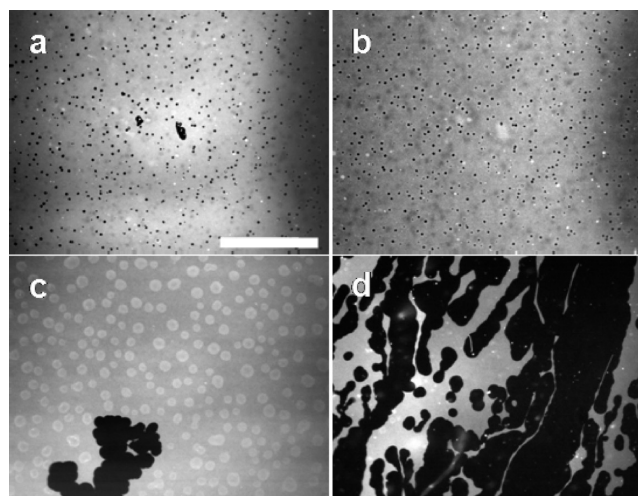


Figure 8. Epifluorescence images of the effect of rinsing the solution above a POPC bilayer back to pH 7.4 PBS buffer. Images are shown before (a and c) and 1 min after rinsing (b and d) for both bilayer exposed to pH 1 (a and b) and pH 13 (c and d) for 10 min (the scale bar represents $40\ \mu\text{m}$).

bilayer shows a large amount of delamination, where much of the bilayer is removed from the surface.

While rinsing with a pH 7.4 PBS buffer solution allowed us to test for reversibility, additional treatment with acidic or basic pH solution was conducted to test if the amount of acid/base was a limiting factor of bilayer reorganization. These experiments were conducted by first exposing a POPC bilayer to either pH 1 or 13 for 10 min and then rinsing with either additional acid or base at the same pH. These experiments produced images similar to those of Figure 8, as additional exposure produced no new reorganization (data not shown).

The role of fluorescence dye was explored by repeated our experiments with Texas Red DHPE instead of C_{12} -Bodipy-PC as

the fluorescent probe. Texas Red DHPE is significantly different than C₁₂-Bodipy-PC as it has a fluorescently labeled headgroup, instead of having a label attached to the acyl chains, as C₁₂-Bodipy-PC does. We found no difference in the reorganization of a POPC bilayer when switching the fluorescent probe from Texas Red DHPE to C₁₂-Bodipy-PC (data not shown). The only difference observed was that the Texas Red DHPE was significantly less photostable under acidic and basic pH conditions.

One final experiment was conducted to examine the possible role of electrostatic forces in the reorganization of a POPC bilayer. Screening of possible electrostatic forces was conducted by adding 500 mM NaCl to all solutions (data not shown). The ionic strength of the solution produces a highly screening environment with a Debye length of $\kappa^{-1} = 0.5$ nm.⁹ Addition of pH 13, 500 mM NaCl solution was sufficient to eliminate the reorganization observed in Figure 4. Epifluorescence images of the bilayer remained a uniform intensity after 1 h exposure to pH 13. Interestingly, we find that when the same concentration of NaCl is added to the pH 1 experiments, there is no significant difference and the reorganization shown in Figure 1 persists.

DISCUSSION

We have used a combination of imaging techniques to show that exposure of a fluid POPC lipid bilayer to extreme acidic and basic environments promotes reorganization of an initially 2D bilayer into 3D structures. In order to identify the possible mechanisms behind the reorganization, we consider the chemical and physical changes to both POPC molecules and the underlying glass substrate.

First we consider how pH affects the glass surface that supports the bilayer. Charging of borosilicate glass, as well as most oxide surfaces, is dependent on the acid/base properties of surface functional groups. On borosilicate glass, the predominate surface moieties are hydroxyl groups bound to Si and B atoms. The isoelectric point of silica, and most glass surfaces, depends on surface composition and is ~ 2 .¹⁰ This implies that in our experiments we may consider the glass surface to be positively charged and negatively charged at acidic and basic pH, respectively. Note that while the lipid bilayer covers the glass surface, we will later discuss that the bilayer is fairly permeable to both H⁺ and OH⁻ ions, allowing the pH above the bilayer to affect the underlying glass.¹¹

Charging of the lipid molecules is also dependent upon the pH of their environment. The lipids used in our experiments have a PC headgroup that is composed of a glycerophosphoric acid and choline. In a simple electrostatic picture, the glycerophosphoric acid can either be negatively charged or electrically neutral with a pK_a of ~ 1 (depending on ionic environment) and choline is a quaternary ammonium cation with a positive charge that is environmentally insensitive.¹² However, a simple protonation/deprotonation model is insufficient to describe the charging of a PC headgroup. Recent electrokinetic measurements have shown that in the pH range of 2–9, the charge of PC lipids is dependent upon adsorption of both OH⁻ and H⁺/H₃O⁺ ions.¹³ The adsorption of these ions is asymmetric in that the lipids exhibit an isoelectric point at pH 4. While, to our best knowledge, there has not been work published regarding the charging of PC lipid at the extreme pH values of our work, we can combine protonation and ion adsorption to estimate the charging of PC lipids under extreme pH. Under exposure to high pH, even though the PC is technically zwitterionic, the average lipid surface acquires net

negative charge through adsorption of OH⁻ ions. In the opposite extreme, lowering the pH below the pK_a of PC creates both positively charged lipid molecules and lipid surface.

Beyond creating charged species, both acids and bases have the potential to catalyze the hydrolysis of many lipids. POPC has the potential to be hydrolyzed in four locations.¹⁴ Both the carboxy esters and phosphate ester bonds are susceptible to cleavage through hydrolysis. We only consider the possible role of carboxy ester hydrolysis, as previous work has shown that they hydrolyze significantly faster than the phosphate esters.¹⁴ Analysis of the reaction rates for hydrolysis of the carboxy esters in PC lipids shows that this reaction proceeds too slowly to be the dominant mechanism in our observed bilayer reorganization. Both acid- and base-catalyzed hydrolysis display pseudo-first-order kinetics with equal probability for each carboxy ester (*sn*-1 and *sn*-2).¹⁴ While few studies have probed the extreme pH conditions of our experiments, the hydrolysis rate at pH 1 has been reported in the range of 10^{-5} – 10^{-6} s⁻¹^{14,15} and at pH 12.7 in the range of 10^{-3} – 10^{-6} s⁻¹.^{14,16} The half-life of these rates is in the range from ~ 20 min to ~ 50 h and varies depending upon temperature, ionic strength, and aggregation state of the lipids. In the context of our experimental time scales, where the bilayer reorganizes in several seconds or less, we believe that hydrolysis is *not* the primary mechanism, nor are hydrolyzed lipids a product of significance, rendering the LBA still mostly a single component. However, from the known reaction rates, we must assume that in our experiments a small percentage of POPC is being hydrolyzed into lyso-PC and the corresponding fatty acid. Both of these products are single-chain surfactants that behave significantly different than double-chain lipids, as they tend to form spherical micelles instead of bilayer structures.^{5,9,17,18} While the creation of the hydrolysis products does not create reorganization of the bilayer, their surfactant nature may help stabilize the reorganized structures by partitioning into regions of high curvature.

Understanding how strongly acidic and basic pH can modify both the lipids and substrate in our experiments allows us to propose a mechanism for how an initially flat bilayer reorganizes into complex 3D geometries. First, consider the reorganization caused by exposure to acidic conditions. The caplike structures observed in Figures 1–3 are reminiscent of the effort by the Hovis lab in characterization of a mixed lipid bilayer system of PC and phosphatidic acid (PA) lipids.^{7,8} In their work, Hovis et al. showed that upon exposure to an asymmetric ionic environment PC/PA mixed lipid bilayers can undergo similar behavior of creation of hemispherical caps that protrude from the bilayer surface. Note that there are several differences between the work of Hovis et al. and that presented here. First is that the previous work was concerned with mixed lipid systems, whereas we show that bilayer reorganization is capable with a single-component bilayer. Second, while caps of PC/PA lipids were never observed to detach from the surface, we clearly observe this to happen. Finally, Hovis et al. does not report evidence of holes or voids formed in LBAs, something observed for all of our samples. Dark spots observed in their images are attributed to dye segregation due to lipid phase separation. However different, the observation of cap formation produces strikingly similar images between the two experiments, and thus, we propose a similar mechanism that requires two components for acid-induced reorganization.

The first component needed to create caps in the bilayer is an asymmetry in the curvature between the outer and inner leaflets

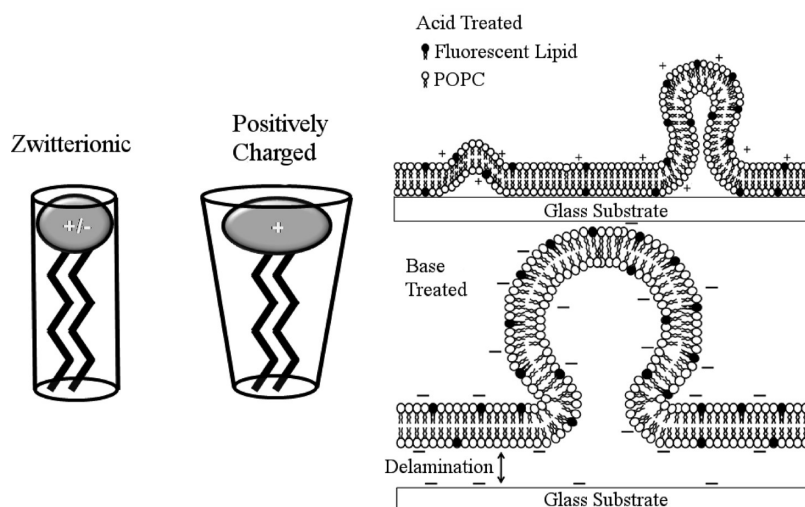


Figure 9. Schematic depicting the mechanism of lipid bilayer reorganization under acidic (top, right) and basic pH (bottom, right). Charging of LBA/glass is represented with the appropriate positive/negative marking. Lipid shape change associated with protonation of POPC is also depicted (left). The zwitterionic state of POPC produces a cylindrical molecule that becomes a truncated-cone upon protonation.

of the bilayer. Creation of caps has been previously predicted to occur in two-phase lipid systems with asymmetric leaflets and is accomplished by protonation of the PC headlet. As discussed above, the isoelectric point of the lipid surface occurs at pH 4.¹³ Below pH 4 the bilayer acquires a net positive charge due to $\text{H}^+/\text{H}_3\text{O}^+$ adsorption. However, it is not until the pH is lowered to the pK_a of the glycerophosphoric acid group (~ 1) that the PC headgroup become protonated.¹² Upon charging from a zwitterion to a net positive charge species, the effective area of the PC headgroup increases due to electrostatic repulsion between other charged headgroups.^{5,9,17} The primary effect of this is that the lipid changes shape from a cylinder to a truncated cone, which promotes a change in the spontaneous curvature of the bilayer.¹⁸ In a simple model considering the packing constraints of lipids it is well established that cone-shaped molecules tend to form curved structures, such as micelles, instead of planar bilayers formed by packing of cylindrically shaped lipids.¹⁸ A schematic of this scenario is depicted in Figure 9. The lipids in the outer leaflet are preferentially charged over the inner as they are directly exposed to the low pH. The observation in Figure 2 that, as the pH is decreased below 1, the process of cap and hole formation is significantly increased supports our conclusion of PC protonation creating leaflet asymmetry. As the pH is decreased further below the pK_a of glycerophosphoric acid, a greater number of lipids protonate; thus, more caps are formed.

A secondary component that is necessary, but not sufficient, to create caps is that the LBA must be in a 2D fluidic phase. The rigid mechanical behavior of the gel-phase DSPC bilayer resists reorganization under these acidic conditions. The energy needed to deform the bilayer is merited in both the bending and area-expansion modulus. Both of these moduli are typically greater by 1 order of magnitude for gel-phase bilayers in comparison to fluid phase.²⁰

Our conclusion that the limiting factor in cap formation is the ability to create an asymmetric distribution of protonated POPC lipids also hints at why caps are observed to sometimes disappear and absorb into the bilayer. To explain this phenomenon, we must consider the permeability of lipid bilayers to passive H^+/OH^- transport. The 1D diffusion constant of these ions through a lipid bilayer is reported to be $10^{-4} \text{ cm s}^{-1}$, nearly as high as water.¹¹ Note

that this measurement is for a patch-clamp geometry in which a lipid bilayer is suspended across a pore, whereas we use a solid-supported LBA geometry. This difference is significant as the hydration layer separating a LBA and its solid support has been estimated to have a significant increase in viscosity ($1000\times$) over that of bulk water.^{21,22} Therefore, while passive H^+/OH^- transport across the LBA occurs in a few microseconds, it may take several seconds for the lateral diffusion of these ions in the hydration layer between the substrate and bottom leaflet of the LBA to reach equilibrium. The significance of high permeability to H^+/OH^- ions is that upon exposure to low pH the leaflet asymmetry in the bilayer is quickly relieved as the thin hydration layer under the bilayer begins to match the pH of the outer solution. As the leaflet asymmetry is reduced, the caps do not have a driving force to bend away from the substrate and begin to lie flat. The ability to form an asymmetric pH environment for two leaflets is also destroyed, on an even greater level, when holes are created in the bilayer through cap removal. When combined, both permeability and hole creation explains why the cap formation ceases after a few seconds, as the system loses the ability to maintain leaflet asymmetry. Rinsing an acid-treated bilayer with additional acid solution also supports this mechanism. Once the bilayer loses the ability to maintain leaflet asymmetry, additional acid does nothing, as it will modify both leaflets at roughly the same rate.

Similar to the work of Hovis et al.,^{7,8} we believe that inhomogeneity in the composition of the bilayer is a final necessary component for cap formation. Any inhomogeneity in composition leads to the creation of discrete regions of leaflet asymmetry, which form caps, as opposed to even distribution of protonated species throughout the outer leaflet. Small changes in composition and structure may also explain why some caps are removed through detachment, while others absorb into the bilayer. While we discussed above that a bilayer is highly permeable to H^+/OH^- ions, the measured diffusion constant is a global average through the entire bilayer. Inhomogeneity also creates regions of the bilayer that are more/less permeable than the global average. In regions of high permeability, the caps absorb; in contrast, regions of low permeability create caps that grow until they detach from the surface.

The final feature observed in acid-induced reorganization of POPC bilayers are the irregularly shaped membrane disruptions observed in Figures 1–3. As caps form during exposure to low pH, the bilayer is able to accommodate them through expansion; however, fluid bilayers are only able to expand a few percent before undergoing membrane lysis.²³ The expansion that a bilayer must accommodate during cap formation can, however, be much larger than a few percent. Considering that a hemispherical cap has twice the surface area of a flat circle of the same dimensions, the cap density observed in Figures 1 and 2 creates a condition where the bilayer is unable to accommodate the cap-induced expansion. Once the bilayer cannot accommodate the expansion, the bilayer tears through lysis and creates the irregularly shaped holes observed in Figures 1–3. This effect is dramatic at pH 0 (Figure 2a), where the bilayer is completely covered with either caps or holes.

Finally, note that at pH <1 both the bilayer and glass are positively charged and there may exist a significant repulsive electrostatic force acting between the two surfaces. We can disregard the role of this force in acid-induced bilayer rearrangement, as addition of 500 mM NaCl to the experiment produced the same reorganization. As mentioned above, the Debye length ($\kappa^{-1} = 0.5$ nm) at this ionic strength indicates that electrostatic interactions are limited to subnanometer ranges.^{9,17}

The structural reorganization of a POPC bilayer caused by highly basic conditions has several distinct differences compared to that of acidic conditions. Most notable is that addition of 500 mM NaCl to the experiment was sufficient to stop bilayer reorganization and that reorganization continues over several hours after the initial exposure. These differences indicate that the mechanism for basic pH induced disruption is different than that for acid.

While we successfully characterized the features produced on a bilayer at longer time scales, we were unable to further investigate the reorganization observed within the first few seconds on exposure to highly basic pH (Figure 4a–e). However, the observation of bright patches that grow, sometimes along with dark spots in the center, is indicative of two possible events. First we consider the possibility of phase separation within the bilayer. To test this hypothesis, we created a mixed bilayer of POPC/DSPC to establish the partitioning behavior of the C₁₂-Bodipy-PC dye.²⁴ This test revealed that C₁₂-Bodipy-PC preferentially partitions in fluid-phase films (see Supporting Information). Considering that a POPC bilayer is an initially fluid-phase film, it is unlikely that the bright patches observed in the first few seconds of base exposure are indicative of creation of an even more fluidic phase. Also note that if phase separation is occurring and dye is being partitioned into highly fluid areas of the bilayer, there must be corresponding areas that are depleted of dye. While we do observe small dark spots on the sample, the total surface coverage of these dark spots is quite small (<1%). Finally, if the bright-colored spots are in fact due to extra dye, the time scale on which these features could grow is limited by the diffusion of the dye within the lipid bilayer. We observe bright patches as large as 1 mm² to be created within 1 s; this is much faster than the typical diffusion time for a dye within a fluid phase lipid bilayer ($\sim 1 \mu\text{m}^2/\text{s}$).^{7,25} For these reasons, we can eliminate base-induced phase separation as a mechanism to produce the images shown in Figures 4–6.

Another possibility is that the bright patches formed with the first few seconds of exposure to high pH are due to large-scale delamination of the bilayer. The delaminated patches may appear

brighter if, during delamination, they move closer to the focal plane of the microscope. Several observations lead us to conclude that the bilayer is delaminating from the surface and becomes effectively *unsupported* within the first few seconds of exposure to highly basic pH.

The first of these observations is highlighted in Figure 4. Upon treatment with pH ≥ 12 we often observe large dark patches, up to ~ 1 mm², that appear and disappear within seconds. As discussed above, characterization of these dark features proved them to be large holes in the bilayer. These holes are similar to those formed during acid treatment when the bilayer is stretched beyond its capacity for expansion, and we believe a similar phenomenon is occurring. As the bilayer delaminates from the surface, it forms a 3D structure with increased surface area. If this expansion is greater than the bilayer can accommodate, it tears and forms a hole, as seen in Figure 4b. As the delaminated patches grow larger, the 3D nature and associated surface area decreases. This process eliminates the expansion-induced stress, and the torn bilayer quickly heals (Figure 4c).

Additional evidence to support bilayer delamination is found with rinsing experiments shown in Figure 8. Rinsing a bilayer exposed to basic conditions for 10 min with either PBS buffer or more of the basic solution causes significant disruption. Once the bilayer becomes unsupported, the shear forces associated with rinsing are enough to destroy the overall bilayer structure, leaving only a small section of the bilayer intact. We are currently investigating strategies to slowly return the bilayer to neutral pH in order to create a stable unsupported bilayer, which would be well-suited for a wide variety of biophysical applications.

After the initial delamination caused by exposure to base, epifluorescence images at longer time scales (Figure 4f–h) indicates that the LBA again reorganizes into 3D structures. These structures are identified in Figure 5a–c as hemispherical caps and dynamically grow and coalesce over a time scale of several minutes to hours. We again observe these 3D structures to be accompanied by creation and healing of large holes in the LBA that are few in number but very large in size (Figure 4g). Both caps and holes grow and shrink in a dynamic interplay that maintains the same overall surface area of the bilayer. As noted, the dynamic behavior of these holes required significant trial and error to image one with AFM. We were only able to successfully characterize one of these holes when one would become fixed in a single location. It is unclear why a few of the dynamic holes become fixed; however, it may be related to defects on glass or around the edges of holes in the bilayer.

One final question is why exposure to basic solutions causes a POPC LBA to delaminate and form the large 3D structure of Figures 4–6. This is answered by again considering charging of each surface due to deprotonation and OH⁻ ion adsorption. Recalling that the isoelectric points of glass and POPC occur at pH ~ 2 and 4, respectively, both surfaces become significantly negatively charged at high pH.^{10,13} While individual POPC molecules may become positively charged through protonation under acidic pH, leading to a change in molecular shape, this is not the case with basic conditions. High pH values do not vary the charge of individual lipids and only changes the net charge of the surface through ion adsorption. Previous work has shown that by pH 9 the ζ -potential of these surfaces is $\zeta = -120$ mV for glass and $\zeta = -80$ mV for POPC.¹³ Note that a surface potential of ± 25 mV is typically regarded as a merit to divide low from highly charged surfaces.¹⁷ Combining the surface charge with previous work establishing that OH⁻ ions easily diffuse across

the LBA and access the bottom leaflet of the bilayer and glass substrate,¹¹ it is clear that significant repulsive electrostatic force builds at the bilayer/glass interface.

Upon exposure to $\text{pH} \geq 12$, the electrostatic repulsion overcomes the combination of hydration, electrostatic, steric, and van der Waals forces that adhere the bilayer to the glass,^{9,26,27} and the bilayer delaminates and becomes unsupported. If this electrostatic repulsion is also large enough to overcome the bending modulus of the bilayer [$\sim(1-10) \times 10^{-19}$ J],^{28,29} the LBA bends away from the substrate and creates large hemispherical caps (Figure 6b) that grow into spherical buds (Figure 6c) and more complex irregularly shaped structures (Figure 4j). The variation of pH shown in Figure 5 shows that at pH 12 the bilayer reorganization stops after the initial delamination and only at $\text{pH} \geq 12.5$ does the electrostatic repulsion become significant enough to induce further reorganization. Note that screening of the electrostatic repulsion can be accomplished by addition of 500 mM NaCl. As discussed earlier, the ionic strength of monovalent salt limits the range of electrostatic interactions to subnanometer lengths. Therefore, exposure to $\text{pH} \geq 12$ with 500 mM NaCl produces no reorganization of the bilayer.

The ability to create complex 3D geometries in a single-component LBA has several important implications. First, the heavy exploration of lipid membranes for biosensor development necessitates understanding the response of lipid membranes in various environmental conditions. Further, our results indicate the potential ability to design biomimetic assemblies with programmable behavior, a desirable trait in biomimetic design. Second, the fundamental behavior of simple one-component systems under extreme environments may help elucidate another mechanism for self-replication and compartmentalization occurred during biogenesis. We demonstrate that extreme pH environments, possibly similar to prebiotic conditions, may induce striking behavior in LBAs that is typically not observed under physiological conditions. Also, to our best knowledge, this work is the first demonstration of creation of large-scale *unsupported* LBAs without an intermediate cushion between the surface and membrane. Utilizing unsupported LBA geometries may prove useful in understanding membrane-associated protein structure–function relationships. These proteins typically exhibit steric hindrance and loss of activity as they interact with substrates in supported LBAs.³⁰ Thus, increasing the bilayer/substrate separation through delamination may mitigate these issues. Lastly, many of the dynamic structures and processes observed, including vesicle budding and dynamic membrane disruption and healing events, can be further studied to provide insight into how these processes occur, much of which is still debated.

CONCLUSIONS

It has been shown that single-component LBAs containing phosphatidylcholine bearing lipids can undergo reorganization from an initially 2D fluid lipid bilayer assembly into an array of 3D structures. Upon exposure to a highly acid environment, the phosphatic acid portion of the lipid molecule becomes protonated, creating an effective shape change of the lipids from cylinders into truncated cones. Packing constraints then force the LBA to bend away from an underlying substrate and form hemispherical caps. Upon reaching a certain size, these caps are removed from the LBA, a process similar to membrane budding. Under exposure to highly basic conditions the LBA and

underlying glass substrates become significantly negatively charged. Electrostatic repulsion between the LBA and substrate creates delamination and significant localized curvature of the membrane. Control over pH-induced LBA reorganization may allow for programmed formation of membrane morphologies for use in membrane-based composite materials, such as biosensors, as well as provide information on membrane biophysical questions.

ASSOCIATED CONTENT

S Supporting Information. Epifluorescence microscopy movies and dye partitioning experiments. This material is available free of charge via the Internet at <http://pubs.acs.org>.

AUTHOR INFORMATION

Corresponding Author

*E-mail: mgoertz@sandia.gov.

ACKNOWLEDGMENT

This work was performed, in part, at the Center for Integrated Nanotechnologies, a U.S. Department of Energy, Office of Basic Energy Sciences user facility. Sandia National Laboratories is a multiprogram laboratory operated by Sandia Corp., a Lockheed-Martin Co., for the U.S. Department of Energy under Contract No. DE-AC04-94AL85000. Los Alamos National Laboratory, an affirmative action equal opportunity employer, is operated by Los Alamos National Security, LLC, for the National Nuclear Security Administration of the U.S. Department of Energy under contract DE-AC52-06NA25396.

REFERENCES

- (1) Alberts, B. *Molecular Biology of the Cell*, 5th ed.; Garland Science: New York, 2008.
- (2) Ponnuswamy, A.; Nulton, J.; Mahaffy, J. M.; Salamon, P.; Frey, T. G.; Baljon, A. R. C. *Phys. Biol.* **2005**, *2* (1), 73–79.
- (3) Hohmann-Marriott, M. F.; Blankenship, R. E. *FEBS Lett.* **2007**, *581* (5), 800–803.
- (4) Eggins, B. R. *Biosensors: An Introduction*; Wiley-Teubner: New York, 1996; p xi.
- (5) Yeagle, P. *The Structure of Biological Membranes*; CRC Press: Boca Raton, FL, 1992.
- (6) Deamer, D.; Singaram, S.; Rajamani, S.; Kompanichenko, V.; Guggenheim, S. *Philos. Trans. R. Soc. B* **2006**, *361* (1474), 1809–1818.
- (7) Cambrea, L. R.; Haque, F.; Schieler, J. L.; Rochet, J. C.; Hovis, J. S. *Biophys. J.* **2007**, *93* (5), 1630–1638.
- (8) Cambrea, L. R.; Hovis, J. S. *Biophys. J.* **2007**, *92* (10), 3587–3594.
- (9) Israelachvili, J. N. *Intermolecular and Surface Forces*, 2nd ed.; Academic Press: London, 1991; p xxi.
- (10) Iler, R. K. *The Chemistry of Silica*; Wiley-Interscience: New York, 1979.
- (11) Gutknecht, J. *J. Membr. Biol.* **1984**, *82* (1), 105–112.
- (12) Tocanne, J. F.; Teissie, J. *Biochim. Biophys. Acta* **1990**, *1031* (1), 111–142.
- (13) Zimmermann, R.; Kuttner, D.; Renner, L.; Kaufmann, M.; Zitzmann, J.; Muller, M.; Werner, C. *Biointerphases* **2009**, *4* (1), 1–6.
- (14) Grit, M.; Crommelin, J. A. *Chem. Phys. Lipids* **1993**, *64* (1–3), 3–18.
- (15) Ho, R. J. Y.; Schmetz, M.; Deamer, D. W. *Lipids* **1987**, *22* (3), 156–158.
- (16) Kensil, C. R.; Dennis, E. A. *Biochemistry* **1981**, *20* (21), 6079–6085.

- (17) Hiemenz, P. C.; Rajagopalan, R. *Principles of Colloid and Surface Chemistry*, 3rd ed.; marcel Dekker: New York, 1997.
- (18) Zimmerberg, J.; Kozlov, M. M. *Nat. Rev. Mol. Cell Biol.* **2006**, *7* (1), 9–19.
- (19) Harden, J. L.; MacKintosh, F. C.; Olmsted, P. D. *Phys. Rev. E* **2005**, *72* (1), 011903.
- (20) Lin, W. C.; Blanchette, C. D.; Ratto, T. V.; Longo, M. L. *Biophys. J.* **2006**, *90* (1), 228–237.
- (21) Kim, J.; Kim, G.; Cremer, P. S. *Langmuir* **2001**, *17* (23), 7255–7260.
- (22) Seu, K. J.; Pandey, A. P.; Haque, F.; Proctor, E. A.; Ribbe, A. E.; Hovis, J. S. *Biophys. J.* **2007**, *92* (7), 2445–2450.
- (23) Needham, D.; Nunn, R. S. *Biophys. J.* **1990**, *58* (4), 997–1009.
- (24) See Supporting Information
- (25) Werner, J. H.; Montano, G. A.; Garcia, A. L.; Zurek, N. A.; Akhadov, E. A.; Lopez, G. P.; Shreve, A. P. *Langmuir* **2009**, *25* (5), 2986–2993.
- (26) Radler, J.; Strey, H.; Sackmann, E. *Langmuir* **1995**, *11* (11), 4539–4548.
- (27) Cremer, P. S.; Boxer, S. G. *J. Phys. Chem. B* **1999**, *103* (13), 2554–2559.
- (28) Kucerka, N.; Liu, Y. F.; Chu, N. J.; Petrache, H. I.; Tristram-Nagle, S. T.; Nagle, J. F. *Biophys. J.* **2005**, *88* (4), 2626–2637.
- (29) Sackmann, E. *FEBS Lett.* **1994**, *346* (1), 3–16.
- (30) Castellana, E. T.; Cremer, P. S. *Surf. Sci. Rep.* **2006**, *61* (10), 429–444.